ELSEVIER

Analytical Formulas for Interfacial Transition Zone Properties

Edward J. Garboczi and Dale P. Bentz
National Institute of Standards and Technology, Building Materials Division, Gaithersburg, Maryland

Two analytical results are presented that are of use to concrete material technologists. Using a model of concrete in which the aggregates are spherical, but with an arbitrary size distribution, a result from statistical geometry can be used to accurately give the total interfacial transition zone (ITZ) volume for any width ITZ and any volume fraction of aggregates. In reality, the ITZ contains a gradient of porosity and therefore a gradient of properties. When only a small volume fraction of aggregates is present (called the dilute limit), it is possible to analytically solve for the effect of the ITZ on the overall concrete properties. This calculation can be carried out for the effective linear elastic moduli, linear electrical conductivity/ionic diffusivity, and linear thermal/moisture shrinkage/expansion. The details of the calculation are summarized and applications described. ADVANCED CEMENT BASED MATERIALS 1997, 6, 99–108. *Published by Elsevier Science Ltd.*

KEY WORDS: Concrete, Interfacial transition zone, Cement, Elastic moduli, Conductivity, Shrinkage

It is now well established experimentally that interfacial transition zones (ITZs) exist around aggregate (rock, sand) particles in concrete. This is mainly because the cement paste matrix is itself particulate. When the cement grains encounter the "wall" of the aggregate, a region of higher porosity near the aggregate surface will appear, due to the "packing" constraints imposed by the aggregate surface [1,2]. Because the average aggregate diameter is much larger than the average cement grain diameter, the aggregates on average will appear locally flat to the cement grains, so the ITZ thickness will depend on the median size of the cement grains, and not on the aggregate size [3]. The median diameter of most cements in common use is around 10 to 30 μm, so this is typically the kind of width one finds associated with ITZs. In the case where the cement grains are of the same order size as the aggregate particles, the whole idea of ITZs, at least in the sense considered in this article, loses its meaning. This case is not considered in this article.

The restrained placement of cement around aggregates results in a gradient of porosity, and therefore a gradient of properties, around each aggregate. The high volume fraction of aggregates in a typical concrete (60% to 75%) means that the spacing between adjacent aggregates is only a few times the typical ITZ thickness. This fact implies that the cement paste in the ITZs can have a significant volume fraction and can be percolated [4] and, therefore, can have a significant effect on properties. Of particular interest are elastic moduli, compressive strength, chloride and sulfate diffusivity, electrical and thermal conductivity, shrinkage, and creep. This article is restricted to the (linear) properties of ionic diffusivity (which mathematically is the same as thermal or electrical conductivity [5,6], elastic moduli, and thermal expansion.

Analytical results are presented for the volume fraction of the ITZ phase in a model where the aggregates are spherical and the ITZ is of uniform thickness, and for the dilute limit of an aggregate surrounded by a gradient of properties.

Formula for Interfacial Transition Zone Volume

Lu and Torquato [7] have recently derived an analytical formula for the statistical geometry of composites that is basically set up to predict the ITZ volume fraction. For a packing of spherical particles in a matrix, where the spheres can have any size distribution, they derived an approximate formula for a quantity they denoted as $ev(r)$. Figure 1 shows a schematic view, in two dimensions (2-D), of the geometry of the problem being considered. If a shell of thickness r is put on every sphere in the packing, the quantity $ev(r)$ is defined as the volume fraction of matrix material that is outside all the spheres and all the shells. Clearly, $ev(r) \rightarrow 0$ as $r \rightarrow \infty$, since eventually the shells will overlap enough to fill up all the remaining matrix material. This function was designed to take into account the overlaps of these

Address correspondence to: Dr. E.J. Garboczi, National Institute of Standards, Building Materials Division, Room B350, Building 226, Gaithersburg, Maryland 20899.
Received January 21, 1997; Accepted July 31, 1997

Published by Elsevier Science Ltd.
655 Avenue of the Americas, New York, NY 10010

ISSN 1065-7355/97/$0.00
PII S1065-7355(97)00032-1

Advn Cem Bas Mat
1997;6:99–108

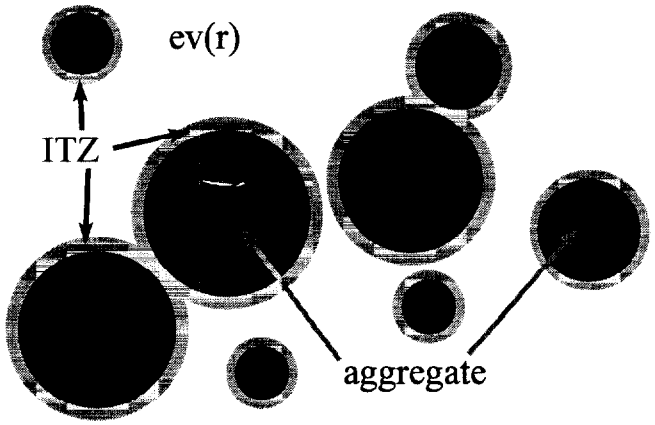

FIGURE 1. Schematic view of the quantities in the Lu and Torquato formula [7]. The thickness of every shell is r.

shells, so as to be accurate not just in the small r limit, where the volume of the shell phase is just the surface area of the particles times r, but for all values of r. In the concrete case, with spherical aggregates, if we take $r = t_{ITZ}$ to be the ITZ thickness, then clearly the ITZ volume fraction is just:

$$V_{ITZ} = 1 - V_{agg} - ev(t_{ITZ}) \tag{1}$$

where V_{agg} is the volume fraction of aggregates in the concrete.

There are certain assumptions that go along with this formula. The aggregate size distribution must be known in terms of the number of particles with a certain size, not the volume of particles with that size. Using some simple assumptions, it is easy to generate this kind of distribution function from a typical sieve analysis. A recent publication gives details of how this can be done [8]. Also, the spherical particles must be in an equilibrium arrangement, that is, arranged as they would be if they were suspended in a liquid and free to move.

Using the result that was derived for $ev(r)$, at $r = t_{ITZ}$, the ITZ volume fraction is then:

$$V_{ITZ} = 1 - V_{agg} - (1 - V_{agg})exp[-\pi\rho(cr + dr^2 + gr^3)] \tag{2}$$

where ρ is the total *number* of particles per unit volume. Using the size distribution function, the quantities c, d, and g in the equation can be defined in terms of the number averages of the particle radius and the particle radius squared:

$$c = \frac{4\langle R^2\rangle}{1 - V_{agg}} \tag{3}$$

$$d = \frac{4\langle R\rangle}{1 - V_{agg}} + \frac{12z_2\langle R^2\rangle}{(1 - V_{agg})^2} \tag{4}$$

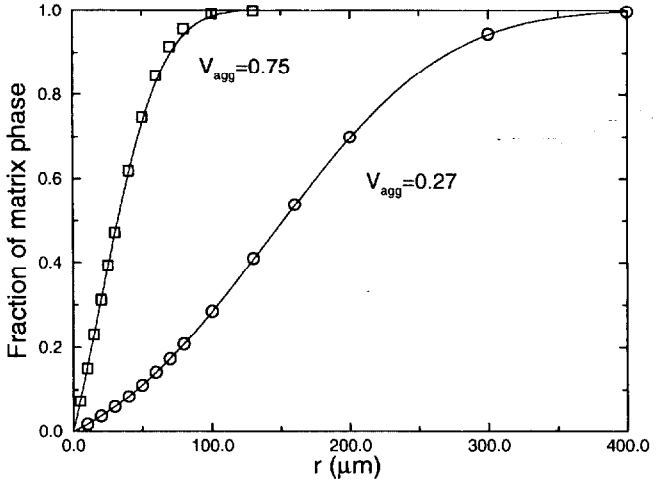

FIGURE 2. Fraction of the matrix phase taken up by the ITZs, of width r, as a function of r, for a typical concrete, at two different aggregate volume fractions, 0.27 and 0.75. The symbols are data points determined by point counting, and the lines are the result from Lu and Torquato's formula [7].

$$g = \frac{4}{3(1 - V_{agg})} + \frac{8z_2\langle R\rangle}{(1 - V_{agg})^2} + \frac{16Az_2^2\langle R^2\rangle}{3(1 - V_{agg})^3} \tag{5}$$

where $z_2 = 2\pi\rho\langle R^2\rangle/3$, A is a parameter equal to 0, 2, or 3, depending on the analytical approximation chosen in the theory [7], and $\langle\ \rangle$ indicates an average over the aggregate size distribution. In all our work on model spherical aggregates, $A = 0$ was always the best choice to use, as decided by comparison to numerically exact model data, although the value of A did not seem to make much difference. The term controlled by the value of A was a small contribution to the prediction of the ITZ volume fraction.

Figure 2 shows a comparison of the above formula to numerical model data for a typical concrete distribution, with aggregate particle sizes ranging from 0.1 to 10 *mm*, which is a range of a factor of 100 in size. Even for distances r that are larger than the usual width of the ITZ, the formula evidently correctly handles the large amount of overlapping of the ITZs, for two different values of V_{agg}, 0.27 and 0.75. Figure 3 shows the same formula applied to a system with 27% by volume of monosize aggregates, where it does not work quite so well. This is because the formula was derived for spherical particles that were arranged like they would be if they were really suspended in a liquid, according to equilibrium statistics. Our models are made by randomly placing spherical particles in the cement paste and not allowing them to move after placement. For monosize particles, it is well known that after about 20% volume fraction of particles are present, the statistics of the two kinds of particle placing gradually become different. If our monosize particles were arranged

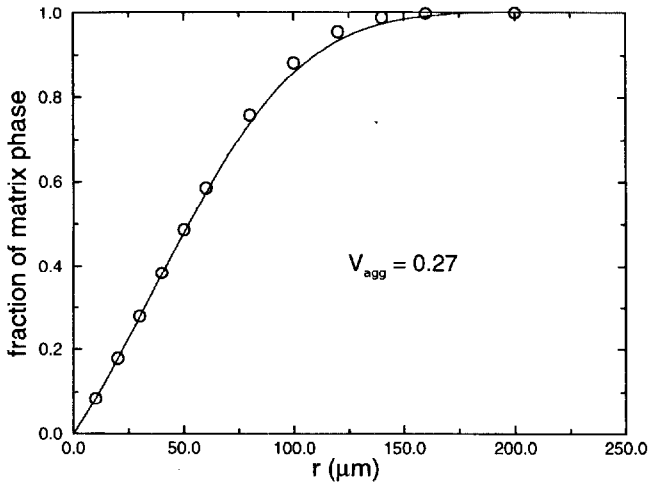

FIGURE 3. Fraction of the matrix phase taken up by the ITZs, of width r, as a function of r, for monosize aggregates, at an aggregate volume fraction of 0.27. The symbols are data points determined by numerical point counting, and the lines are the result from Lu and Torquato's formula [7].

according to equilibrium statistics, then the formula would agree with numerically exact model data to better than 1% accuracy [8]. So, in Figure 3, our system does not meet the conditions necessary for the analytical formula of eq 2 to hold, although the agreement between theory and model is still quite good, especially for the usual ITZ thickness values (10 to 40 μm).

In principle, the formula should not apply to our models for the reason given above. However, somewhat surprisingly, for a very wide particle size distribution, the statistics of the two kinds of particle placing are seemingly almost the same, as the formula fits the typical concrete distribution extremely well (Figure 2). This is an interesting result and deserves closer study to determine under what conditions the statistics of the two different particle arrangements become nearly the same. Experimentally, the aggregates in a concrete are probably in a close-to-equilibrium arrangement, if gravitational settling is not too important, there is a wide size distribution of aggregates, and the aggregates are reasonably spherical. Therefore, the formula should work well in real concrete as long as these conditions are met.

Mathematical Analysis of Dilute Limit for Diffusivity/Conductivity

The dilute limit of a concrete composite occurs when the aggregates are present at a very small volume fraction, so that the effect of each of the aggregates can be treated independently, without any contribution from each other. In this limit, an overall property, P, normalized by the bulk property in the absence of aggregates, P_{bulk}, is given by:

$$\frac{P}{P_{bulk}} = 1 + \langle m \rangle c + O(c^2) + \ldots \tag{6}$$

where c is the volume fraction of aggregates present, and $\langle m \rangle$ is a dimensionless number determined by the aggregate shape, size distribution, the ratio of P_{agg}/P_{bulk}, and the geometrical and physical properties of the ITZ. The angular brackets indicate an average over the size distribution of the aggregates. As an example, for the special case of a spherical aggregate of radius r and zero diffusivity, surrounded by an ITZ of thickness t_{ITZ} and diffusivity D_{ITZ}, embedded in a matrix of diffusivity D_{bulk}, the exact result for m can be found [9,10]:

$$m = (3\alpha)\frac{2(\alpha - 1)\dfrac{D_{ITZ}}{D_{bulk}} - (1 + 2\alpha)}{2(\alpha - 1)\dfrac{D_{ITZ}}{D_{bulk}} + (1 + 2\alpha)} \tag{7}$$

where the parameter $\alpha = [(r + t_{ITZ})/r]^3$ contains all the dependence on the particle and ITZ geometry. In real concrete, the ITZ has a gradient of properties, which is treated in this article. In the following, cases where P is either the bulk modulus, the shear modulus, the thermal expansion coefficient, or the electrical conductivity/ionic diffusivity will be discussed.

If the problem can be worked out where the spherical aggregate is surrounded by N shells of general thickness and properties, then any type of gradient of properties can be handled simply by using as many shells as necessary to mimic the gradient function. The following derivations make use of an idea originally developed for the equivalent elastic problem, that of a transfer matrix approach [11]. The bulk modulus [12] and the Stokes friction and intrinsic viscosity [13] have also been found in the case where the gradient of properties takes on a specific power law form. The simplest case, electrical conductivity/ionic diffusivity, is discussed first.

Figure 4 shows the geometry of the problem for all the properties to be considered, where the inner sphere, which represents the aggregate, is counted as number 1. Then the radius of the aggregate is R_1, the radius of the first shell is R_2, and so on, with the radius of the last shell being R_N. The multilayered inclusion is embedded in matrix material labeled $N + 1$.

We will use conductivity language to do the derivation, with the understanding that electric fields are equivalent to concentration and thermal gradients, and electrical conductivities to ionic diffusivities and thermal conductivities. We want to apply an electric field in the z direction and work out the effective conductivity

Advn Cem Bas Mat
1997;6:99–108

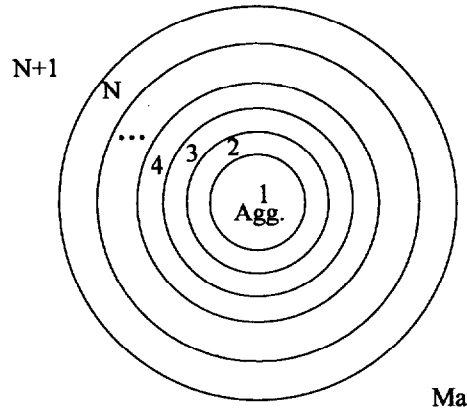

FIGURE 4. Schematic sketch of the geometry of the problem. Each shell is a spherical shell, of radius R_n for the nth shell.

of the multilayered inclusion embedded in the matrix. It does not matter in which direction the field is applied, as the sphere and the spherical shells are isotropic. Let the conductivity of the nth shell be σ_n. With a uniform electric field of strength E_0 in the z direction, the potential far away from the inclusion must be:

$$V = -E_0 z = -E_0 r\cos(\theta) \tag{8}$$

where the usual spherical coordinates (r, θ, ϕ) are used. Laplace's equation for steady-state conduction must be satisfied, $\nabla^2 V = 0$, with the boundary conditions that the potential and normal electrical current are continuous across each of the N boundaries. This gives $2N$ conditions that must be satisfied. The potential in the nth phase can be shown to be of the form:

$$V_n = \left(-A_n r + \frac{B_n}{r^2}\right)\cos(\theta). \tag{9}$$

Two more boundary conditions are that in the aggregate, $B_1 = 0$, since the potential cannot diverge at r = 0, and in the $(N + 1)$th phase, which is the matrix, $A_{N+1} = E_0$, in order to give the correct uniform field far from the aggregate. This results in only $2N$ unknown coefficients, which can be determined uniquely from the $2N$ boundary condition equations.

At $r = R_n$, the boundary between the nth and the (n + 1)th phase, the two boundary conditions can be expressed as:

$$-A_n + \frac{B_n}{R_n^3} = -A_{n+1} + \frac{B_{n+1}}{R_n^3} \tag{10}$$

$$\sigma_n A_n + \frac{2\sigma B_n}{R_n^3} = \sigma_{n+1} A_{n+1} + \frac{2\sigma_{n+1} B_{n+1}}{R_n^3}. \tag{11}$$

By rearranging this equation, one can come up with the form:

$$\begin{pmatrix} A_{n+1} \\ B_{n+1} \end{pmatrix} = P_n \begin{pmatrix} A_n \\ B_n \end{pmatrix} \tag{12}$$

where P_n is a 2×2 matrix, given by:

$$P_n = \frac{1}{3\sigma_{n+1}} \begin{pmatrix} \sigma_n + 2\sigma_{n+1} & 2(\sigma_n - \sigma_{n+1}) R_n^{-3} \\ (\sigma_n - \sigma_{n+1}) R_n^3 & 2\sigma_n + \sigma_{n+1} \end{pmatrix}. \tag{13}$$

By iterating eq 12, one can then derive the equation connecting A_1 and B_1 to A_{N+1} and B_{N+1}:

$$\begin{pmatrix} A_{N+1} \\ B_{N+1} \end{pmatrix} = P_N P_{N-1} \ldots P_3 P_2 P_1 \begin{pmatrix} A_1 \\ B_1 \end{pmatrix} = H \begin{pmatrix} A_1 \\ B_1 \end{pmatrix}. \tag{14}$$

Equation 14 is really two equations in four unknowns, A_{N+1}, B_{N+1}, A_1, and B_1, with the known coefficients H_{11}, H_{12}, H_{21}, and H_{22}. However, since $A_{N+1} = E_0$, and $B_1 = 0$, there are really only two unknowns, so that eq 14 may be easily solved, once the elements of the matrix H have been computed, to give:

$$A_1 = \frac{E_0}{H_{11}}, \; B_{N+1} = \frac{H_{21} E_0}{H_{11}}. \tag{15}$$

Again iterating on eq 12, one can then solve for any of the other coefficients desired.

To get the slope m, one must still derive the effective conductivity, which involves averages over the entire inclusion, of electric field and current. The following equations are completely general for the overall field and current averages:

$$\langle j \rangle \equiv \sigma E_0 = c_I \langle j \rangle_I + (1 - c_I) \langle j \rangle_{N+1} \tag{16}$$

$$\langle E \rangle = E_0 = c_I \langle E \rangle_I + (1 - c_I) \langle E \rangle_{N+1} \tag{17}$$

where I stands for the entire inclusion, aggregate plus $N - 1$ layers, c_I is the volume fraction of the entire inclusion, and σ is the effective conductivity of the entire composite system, treating it as a uniform medium. Combining these two equations so as to eliminate the average over the $N + 1$ phase [14], and using the fact that the volume fraction of aggregate, c, is in the dilute limit given by $c = c_I (R_1/R_N)^3$, we obtain, with the help of eqs 12 to 15:

$$\frac{\sigma}{\sigma_{N+1}} = 1 + \frac{R_N^3}{R_1^3} c \left(\frac{\langle j \rangle_I}{\sigma_{N+1} E_0} - \frac{\langle E \rangle_I}{E_0} \right) \tag{18}$$

$$\langle j \rangle_I = \sigma_{N+1} E_0 \left(1 + \frac{2H_{21}}{R_N^3 H_{11}} \right) \tag{19}$$

$$\langle E \rangle_I = E_0\left(1 - \frac{H_{21}}{R_N^3 H_{11}}\right) \tag{20}$$

so that the final result for the slope m, according to the form of eq 6 is:

$$\frac{\sigma}{\sigma_{N+1}} = 1 + \left(\frac{3H_{21}}{R_1^3 H_{11}}\right) c + O(c^2) \tag{21}$$

$$\langle m \rangle = \frac{3H_{21}}{R_1^3 H_{11}}. \tag{22}$$

Mathematical Analysis of Dilute Limit for Bulk and Shear Moduli

One can perform the same analysis for the bulk modulus. First it is important to recall that for an isotropic linear elastic material, with bulk modulus K, the following equation holds:

$$Tr\ \sigma = 3K\ Tr\ \epsilon \tag{23}$$

where Tr indicates a trace (sum over the diagonal elements) of the stress or strain tensor. We use the same geometrical setup as in Figure 4, again with spherical polar coordinates. The displacement at $r \to \infty$ is $\epsilon_0 r$, a pure compression. Because of the radial symmetry, the only nonzero displacement throughout the structure is $u = u(r)$, the radial component of the displacement vector. There are no shear strains in this case either, and the principal strains are $\epsilon_{rr} = \partial u/\partial r$, $\epsilon_{\theta\theta} = u/r$, and $\epsilon_{\phi\phi} = u/r$. The radial displacement u can be expressed as:

$$u(r) = A_n r + \frac{B_n}{r^2} \tag{24}$$

where A_n and B_n are arbitrary constants in the nth shell. In order to satisfy the boundary condition at $r \to \infty$, $A_{N+1} = \epsilon_0$. In order to have a finite displacement at the center of the aggregate, $B_1 = 0$. Using eq 24 for the displacements and the definitions of the various strains given above, the radial stress in the nth layer is then:

$$\sigma_r = 3K_n A_n - \frac{4G_n B_n}{r^3}. \tag{25}$$

Between each layer, the displacement and the normal or radial stress must be continuous. When N layers are present, this gives $2N$ boundary conditions, plus the two boundary conditions at the origin and at infinity. These $2N + 2$ boundary conditions are enough to determine the $2N + 2$ unknown coefficients. After a little rearrangement, the boundary conditions between the nth and $(n + 1)$th layers can be written in matrix form as:

$$\begin{pmatrix} A_{n+1} \\ B_{n+1} \end{pmatrix} = P_n \begin{pmatrix} A_n \\ B_n \end{pmatrix} \tag{26}$$

where P_n is a 2×2 matrix, given by:

$$P_n = \frac{1}{3K_{n+1} + 4G_{n+1}} \times \begin{pmatrix} 3K_n + 4G_{n+1} & 4(G_{n+1} - G_n)R_n^{-3} \\ 3(K_{n+1} - K_n)R_n^3 & 3K_{n+1} + 4G_n \end{pmatrix}. \tag{27}$$

Following the same steps as for the electrical case, we find that:

$$A_1 = \frac{\epsilon_0}{H_{11}},\ B_{N+1} = \frac{H_{21}\epsilon_0}{H_{11}}. \tag{28}$$

All the layer displacements can now be determined using the boundary conditions and the two known coefficients. To get the actual change in bulk modulus caused by the presence of the aggregates and the gradient of properties around it, we need to again write out the averages over the phases as was done for the electrical/diffusive case. Again, in general, we have:

$$\langle Tr\sigma \rangle \equiv 9K\epsilon_0 = c_I \langle Tr\ \sigma \rangle_I + (1 - c_I)\langle Tr\ \sigma \rangle_m \tag{29}$$

$$\langle Tr\ \epsilon \rangle = 3\epsilon_0 = c_I \langle Tr\ \epsilon \rangle_I + (1 - c_I)\langle Tr\ \epsilon \rangle_m. \tag{30}$$

Using eqs 24 to 28 above, it can be shown that:

$$\langle Tr\ \sigma \rangle_I = 9\epsilon_0\left(K_{N+1} - \frac{4G_{N+1}H_{21}}{3H_{11}R_N^3}\right) \tag{31}$$

$$\langle Tr\ \epsilon \rangle_I = 3\epsilon_0\left(1 + \frac{H_{21}}{H_{11}R_N^3}\right). \tag{32}$$

Putting eqs 29 to 32 together gives the final result:

$$\frac{K}{K_{N+1}} = 1 - \left(\frac{\left(K_{N+1} + \frac{4}{3}G_{N+1}\right)H_{21}}{H_{11}R_1^3}\right) c + O(c^2). \tag{33}$$

The effective shear modulus can be determined in exactly the same way by applying a uniform shear strain at infinity, except that there are now four unknown coefficients that determine the displacements in each layer, because we no longer have radial symmetry due to the applied shear strain. The matrix that connects the coefficients in one layer to those in the next is then

a 4 × 4 matrix. The product of all these matrices produces a matrix that connects the coefficients in the outer layer to the coefficients in the inner layer. One coefficient in the outer layer and two in the inner layer are forced to zero, however, because of having a finite displacement at $r = 0$ and a finite strain at $r \to \infty$, and one coefficient in the outer layer is determined by the applied strain at $r \to \infty$. Therefore, the matrix equation is transformed to only being four equations in four unknowns, rather than being four equations in eight unknowns. Further details of the shear modulus determination can be found in reference [11]. We emphasize that the pattern of solution is the same as for the bulk modulus, but just requiring more algebra. The explicit solution of the shear modulus dilute limit, along with computer programs for the implementation of the equations, will be given in reference [15]. Reference [15] will also contain more details on all the dilute limit work described in this article, as well as discussion of many other exact results from composite theory. This manual will be available online in the near future. It will describe how to use several finite element and finite difference computer codes for determining electrical and elastic properties of random systems. The manual will also describe the operation of computer codes that implement the dilute limits described in this article.

Mathematical Analysis of Dilute Limit for Thermal Expansion

The case of thermal expansion, in the linear regime, is handled using a modified stress-strain equation:

$$\sigma_i = C_{ij}(\epsilon_j - e_j) \tag{34}$$

where C_{ij} is the elastic modulus tensor, the volumetric expansion terms are $e_1 = e_2 = e_3 = e$, and the shear terms are $e_4 = e_5 = e_6 = 0$. In the case of thermal expansion, e would be proportional to temperature, while in the case of moisture-induced expansion or shrinkage, e would depend on relative humidity [16]. The usual Voigt notation is used, where 1 = xx, 2 = yy, 3 = zz, 4 = xz, 5 = yz, and 6 = xy.

The geometry is the same as for the previous cases, except that now we introduce R_{N+1} as being the radius of the outermost layer of the matrix-plus-inclusion system. For free expansion, we need to take the normal stress to be equal to zero at this boundary. There is no applied strain at infinity, so some other condition is needed to be able to determine the problem. The case where the inclusion stops at $r = R_N$, and $R_{N+1} \gg R_N$, is the dilute case, since the volume fraction of aggregate will be $c = R_1^3/R_{N+1}^3 \ll 1$. Again, the only displacement is the radial displacement, and the same form is assumed for the displacement in each shell. All notation is the same as the bulk modulus case. The continuity of the displacement is also identical to the case of the bulk modulus, but now, with the extra thermal expansion terms present in the stress strain relationship, the radial stress in the nth layer becomes:

$$\sigma_r = 3K_n(A_n - e_n) - \frac{4G_nB_n}{r^3} \tag{35}$$

where e_n is the linear expansion of the nth layer.

The equation connecting the coefficients in the $(n + 1)$th layer to those in the nth layer is then somewhat different from the bulk modulus case as well:

$$\begin{pmatrix} A_{n+1} \\ B_{n+1} \end{pmatrix} = P_n \begin{pmatrix} A_n \\ B_n \end{pmatrix} + Z_n \tag{36}$$

where Z_n is a vector of the form:

$$Z_n = \frac{K_{n+1}e_{n+1} - k_ne_n}{K_{n+1} + \frac{4}{3}G_{n+1}} \begin{pmatrix} 1 \\ -R_n^3 \end{pmatrix}. \tag{37}$$

Now, this equation can be iterated to connect the $n = 1$ coefficients to the $n = N + 1$ coefficients. Care must be taken when iterating, as the resulting expression is more complicated than in the bulk modulus case, because of the presence of the Z_n terms. The result is:

$$\begin{pmatrix} A_{N+1} \\ B_{N+1} \end{pmatrix} = P_NP_{N-1} \ldots P_3P_2P_1 \begin{pmatrix} A_1 \\ B_1 \end{pmatrix} + \sum_{m=1}^{N-1} (P_NP_{N-1} \ldots P_{m+1})Z_m + Z_N \tag{38}$$

which then can be written as:

$$\begin{pmatrix} A_{N+1} \\ B_{N+1} \end{pmatrix} = H \begin{pmatrix} A_1 \\ B_1 \end{pmatrix} + Q. \tag{39}$$

Using the fact that $B_1 = 0$ and A_{N+1} and B_{N+1} are related via the zero stress condition at R_{N+1}, this equation becomes two linear equations for two variables, A_{N+1} and A_1. These two variables are then:

$$A_{N+1} = \frac{\frac{3K_{N+1}R_{N+1}^3e_{N+1}}{4G_{N+1}} + Q_2 - \frac{H_{21}Q_1}{H_{11}}}{\frac{3K_{N+1}R_{N+1}^3}{4G_{N+1}} - \frac{H_{21}}{H_{11}}} \tag{40}$$

and

$$A_1 = \frac{A_{N+1} - Q_1}{H_{11}}. \tag{41}$$

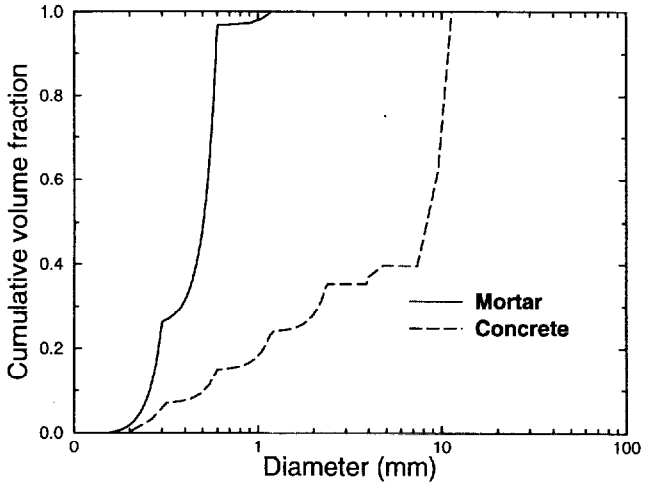

FIGURE 5. Two aggregate particle size distribution functions, in terms of volume, for a C-109 mortar and a typical concrete.

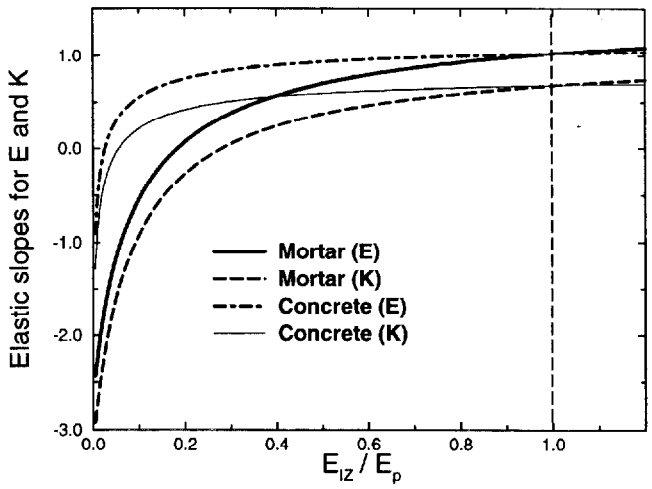

FIGURE 6. Initial slopes for Young's modulus E and bulk modulus K for the mortar and concrete shown in Figure 5.

The overall thermal expansion is then just how much the size of the system has changed, so that the effective thermal expansion, e_{tot}, is the displacement at $r = R_{N+1}$ divided by the original radius of the complete system, R_{N+1}:

$$e_{tot} = \left(A_{N+1}R_{N+1} + \frac{B_{N+1}}{R_{N+1}^2} \right) / R_{N+1} = A_{N+1} + \frac{B_{N+1}}{R_{N+1}^3}. \tag{42}$$

Discussion

What is the use of these exact expressions? First consider the ITZ volume fraction formula. If we take the ITZs as single thickness layers, then this formula gives the total volume occupied by ITZs, taking into consideration the many, possibly multiple, overlaps of this phase. This formula can also be used, as in Figures 2 and 3, to give the matrix volume that is contained within a certain distance of an aggregate surface. For surface controlled phenomena, possibly including alkali-aggregate reaction, for example, this might be an important kinetic parameter. Freeze-thaw damage to the aggregate, for a porous aggregate, might also depend on the distance water has to move from the paste to the nearest aggregate surface. Also, the protected paste for a given air-void system, where the air-voids are the spherical particles, can be investigated with this formula [17].

The exact dilute limit calculations can be applied in several ways. (1) They give a nontrivial, exact calculation of how ITZ properties can affect overall concrete properties. Real concretes have high volume fractions of aggregates, but the qualitative effect of the ITZ can be seen in the dilute case. Since the exact dilute limit is averaged over the volume distribution of the aggregates, differences can be seen, for instance, between mortars and concretes. (2) These formulas serve as useful checks on approximate analytical formulas that are either derived theoretically, in some effective medium approach, or experimentally, by fitting data or by using some other approximate approach. In the dilute limit, these kinds of expressions, if the assumption of a spherical aggregate is used, must reduce to the exact dilute limit formula [8]. (3) It is often easier to think of the ITZ as a zone of some thickness that has a uniform property throughout, rather than as having a gradient of properties. Solving for the exact gradient, then mapping onto the exact solution for a single layer, can give the correct uniform property to be used for a given thickness [18]. (4) Exact dilute limit calculations are, in general, very useful for checking the accuracy of various numerical schemes that attempt to handle the full volume fraction of aggregates [15]. (5) Effective medium theories can be built out of the exact dilute limits in various ways. These effective medium theories can be quite accurate in analyzing the properties of concrete models [8].

Figures 5 and 6 show an example of application (1) above. In Figure 5, the particle size distribution, in terms of the particle volumes, is shown for a C-109 mortar [19] and for a typical concrete [20]. Notice that both go down to about 0.1-mm diameter particles, but the concrete also has particles in the 10-mm range, while the mortar stops at about 1 mm. If there were no ITZ, then the slopes for the mortar and concrete would be identical, as there is no size dependence for the initial slope for a spherical particle embedded in a matrix [21,22], and positive, as the aggregate particle being introduced into the cement paste is stiffer than the

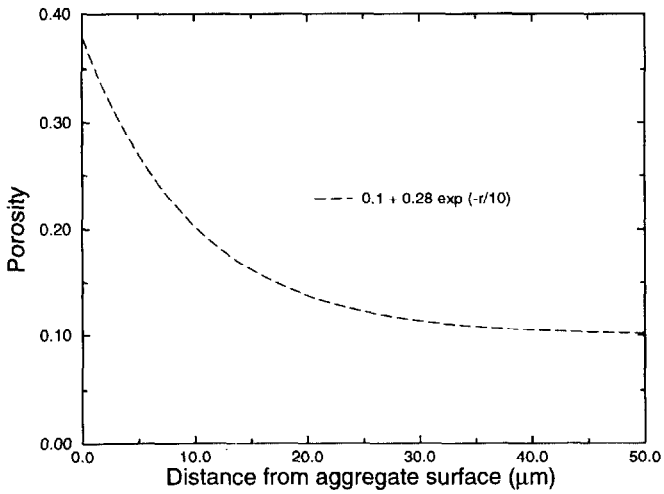

FIGURE 7. Artificial porosity gradient surrounding a spherical particle of diameter 400 μm. The gradient is reminiscent of those found in real concretes.

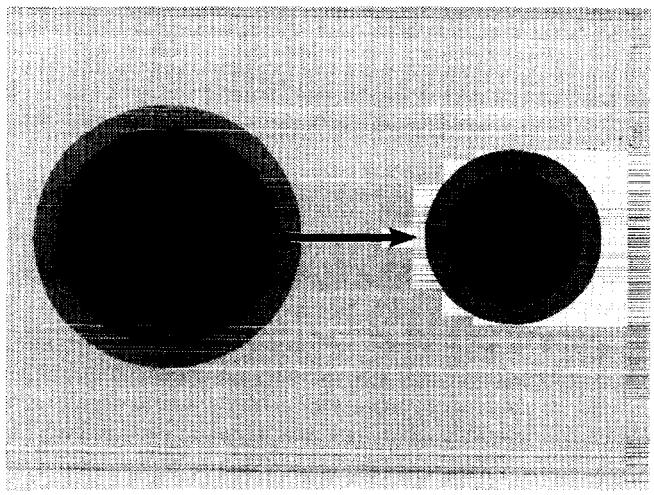

FIGURE 8. Schematic picture showing how the dilute limit of an aggregate surrounded by a gradient in properties can be mapped into the case of an aggregate surrounded by a shell having a given thickness and uniform property.

cement paste. This can be clearly seen in Figure 6 at the point where the Young's modulus of the ITZ equals the Young's modulus of the bulk paste, effectively removing the ITZ. When the ITZ Young's modulus is less than that of the bulk paste, as would be expected because of its higher porosity, then it is clear that the mortar is more affected than the concrete, because of its smaller average diameter. One way of thinking of this is that the smaller the particle, the higher is the ratio of ITZ volume to particle volume. This ratio, for single spherical particles, is $(1 + t_{ITZ}/r)^3$. Alternatively, for the same volume of aggregates, the mortar will have a higher surface area and therefore a higher volume fraction of ITZ than will the concrete. In Figure 6, the bulk and shear modulus of the paste were 20.8 and 11.3, respectively, and the bulk and shear modulus of the aggregate were 44 and 37, respectively, in units of GPa. These values were taken from a case in Zimmerman et al. [23]. The ITZ paste had the same Poisson's ratio as the bulk paste but a smaller Young's modulus as shown in Figure 6.

In an example of application (3), Figure 7 shows a porosity gradient that might be found in a concrete or mortar. The "width" of the ITZ is about 10 μm. We then use the dilute limits to quantitatively map the true dilute limit, for this gradient and a given functional dependence of the properties on the porosity, onto the single uniform property shell case. This mapping is schematically shown in Figure 8. We choose the following sets of properties: σ_p is the electrical conductivity of the bulk cement paste, $\sigma_{agg} = 0$ is the electrical conductivity of the aggregate, and the electrical conductivity of the cement paste in the ITZ scales as the square of the porosity, matching onto σ_p as the distance from the aggregate surface increases. In the elastic moduli case, we take K,G = 10,6 for the aggregate, and K,G = 3,1 for the bulk cement paste, both in arbitrary units. In calculating the bulk modulus slope, the units cancel out anyway. The ITZ cement paste has the same Poisson's ratio as the bulk cement paste, but its Young's modulus scales as the solid fraction cubed [24]. It is important to remember that we are mapping an exact result, for the porosity gradient, onto another exact result, that for a single ITZ shell (N = 3).

Figure 9 shows the electrical conductivity results. It is clear that choosing a larger thickness for the ITZ results in a smaller value of the ITZ conductivity relative to the bulk paste conductivity. In this sense, one cannot really

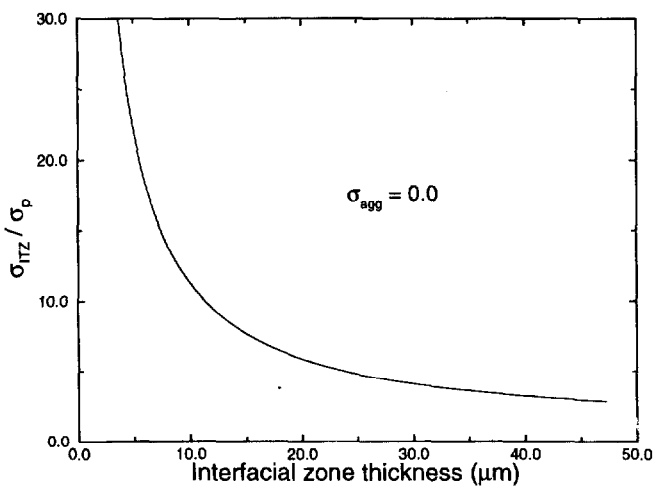

FIGURE 9. Dependence of the ITZ conductivity, compared to the bulk paste conductivity, for various thicknesses of the ITZ.

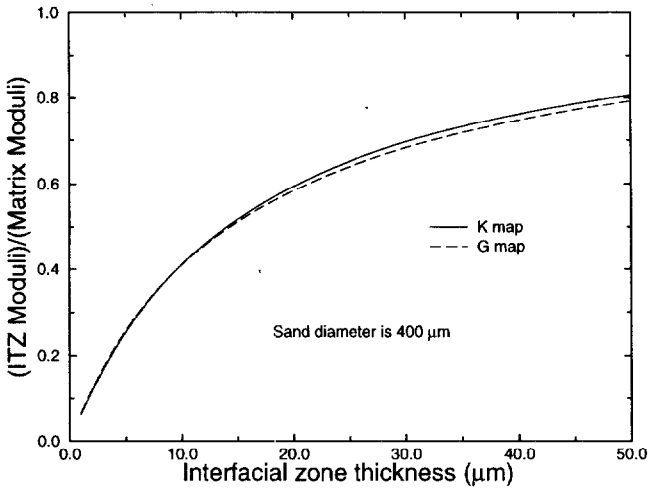

FIGURE 10. Dependence of the ITZ moduli, compared to the bulk paste moduli, for difference thicknesses of the ITZ. The ITZ moduli are chosen so as to have the same Poisson's ratio as the bulk paste. The two curves are generated by matching the bulk modulus slope and the shear modulus slope independently to the true slope generated by the gradient of properties.

talk about "the ITZ conductivity" without specifying the value that is chosen for the thickness. Other articles have suggested that the median diameter of the cement grains should be chosen as the "best" value for the ITZ thickness [8]. The point of Figure 9 is that, if the ITZ is modeled as a uniform property region of some conductivity, this conductivity depends on what thickness is chosen to represent the actual porosity gradient.

Figure 10 shows the elastic results for a similar kind of problem. In the elastic case, the mapping can be done two different ways. The exact bulk modulus slope, for the porosity gradient, can be mapped onto the bulk modulus slope of the single ITZ shell case. This can also be done, with equal validity, using the shear modulus. Figure 10 assures us that, in least in this case, and when the ITZ moduli have the same Poisson's ratio as the bulk paste, essentially the same result is obtained using either the bulk or the shear modulus. As the thickness of the ITZ is increased, the ITZ moduli become larger and therefore closer to the bulk paste moduli. This is because, in the elastic case, the effect of increasing porosity is to make the moduli smaller, so that the ITZ moduli are less than the bulk values, and increase with distance away from the aggregate surface. This is the exact opposite of the case for the conductivity.

Summary

For spherical aggregates, of any size distribution, an analytical formula has been presented, taken from the statistical geometry of composites literature, which very accurately gives the total volume that lies within a distance r of an aggregate surface. This can be used to predict the ITZ volume in concrete. For a spherical aggregate, surrounded by a radially symmetric gradient in properties, it has been shown how to solve exactly for the effective concrete property in the dilute limit, where there is only <5% by volume of aggregate. The properties solved for are electrical conductivity and ionic diffusivity, linear elastic moduli, and linear thermal and moisture-driven expansion and shrinkage. Both of these results should be of use to experimentalists and modelers in the field of cement based materials.

Acknowledgments

The authors wish to acknowledge support from the National Science Foundation Science and Technology Center for Advanced Cement-Based Materials, and from the NIST High-Performance Construction Materials and Systems Program.

References

1. Scrivener, K.L. In *Materials Science of Concrete, Vol. I*; Skalny, J., Ed.; American Ceramic Society: Westerville, OH, 1989; pp 127–161.
2. Garboczi, E.J.; Bentz, D.P. *J. Mater. Res.* **1991,** *6,* 196–208.
3. Bentz, D.P.; Garboczi, E.J.; Stutzman, P.E. In *Interfaces in Cementitious Composites*; Maso, J.C., Ed.; **1992,** *18,* 107–116.
4. Winslow, D.N.; Cohen, M.D.; Bentz, D.P.; Snyder, K.A.; Garboczi, E.J. *Cem. Concr. Res.* **1994,** *24,* 25–37.
5. Douglas, J.F.; Garboczi, E.J. *Adv. Chem. Phys.* **1995,** *91,* 85–153.
6. Garboczi, E.J.; Douglas, J.F. *Phys. Rev. E* **1996,** *53,* 6169–6180.
7. Lu, B.; Torquato, S. *Phys. Rev. A* **1992,** *45,* 5530–5544.
8. Garboczi, E.J.; Bentz, D.P. *J. Adv. Cem. Based Mater.* **1997** (In press).
9. Garboczi, E.J.; Schwartz, L.M.; Bentz, D.P. *J. Adv. Cem. Based Mater.* **1995,** *2,* 169–181.
10. Schwartz, L.M.; Garboczi, E.J.; Bentz, D.P. *J. Appl. Phys.* **1995,** *78,* 5898–5908.
11. Herve, E.; Zaoui, A. *Int. J. Eng. Sci.* **1993,** *31,* 1–10.
12. Lutz, M.P.; Monteiro, P.J.M. In *Microstructure of Cement-Based Systems/Bonding and Interfaces in Cementitious Materials,* Vol. 370; Diamond, S.; Mindess, S.; Glasser, F.P.; Roberts, L.W.; Skalny, J.P.; Wakeley, L.D.; Eds.; Materials Research Society: Pittsburgh, 1995; pp 413–418.
13. Broersma, S. *J. Chem. Phys.* **1958,** *28,* 1158–1168.
14. Hashin, Z. *J. Comp. Mater.* **1968,** *2,* 284–300.
15. Garboczi, E.J. Finite element and finite difference codes for computing the linear electrical and elastic properties of digital images of random materials. *NIST Internal Report,* 1997 (In press). Also at [http://ciks.cbt.nist.gov/garboczi/].
16. Hashin, Z. *J. Appl. Mech.* **1983,** *50,* 481–505.
17. Snyder, K.A. Unpublished data.
18. Garboczi, E.J.; Bentz, D.P. ASCE 4th Materials Conference Proceedings, Washington DC, November 1996.

Advn Cem Bas Mat
1997;6:99–108

19. ASTM C-109 specification. In *Annual Book of ASTM Standards, Vol. 04.02. Concrete and Aggregates*; ASTM: Philadelphia, PA, 1993.
20. Winslow, D.N.; Liu, D. *Cem. Concr. Res.* **1990,** *20,* 227.
21. Neubauer, C.M.; Jennings, H.M.; Garboczi, E.J. *J. Adv. Cem. Based Mater.* **1996,** *4,* 6–20.
22. Christensen, R.M. *Mechanics of Composite Materials*; Krieger Publishing Co.: Malabar, FL, 1991.
23. Zimmerman, R.W.; King, M.S.; Monteiro, P.J.M. *Cem. Concr. Res.* **1986,** *16,* 239–245.
24. Helmuth, R.A.; Turk, D.H. *Highw. Res. Board Spec. Rep.* **1966,** *90,* 135–144.